Simmons, Daniel and Cools, Kristof and Sewell, Phillip (2015) Coupling of unstructured TLM and BEM for accurate 2D electromagnetic simulation. In: International Conference on Electromagnetics in Advanced Applications (ICEAA) 2015, 7-11 Sept. 2015, Turin, Italy.

Coupling of Unstructured TLM and BEM for Accurate 2D Electromagnetic Simulation

D. Simmons* K. Cools* P. Sewell*

Abstract — **In this paper the hybridisation of the 2D time-domain boundary element method (BEM) with the unstructured transmission line method (UTLM) will be introduced, which enables accurate modeling of radiating boundary conditions and plane wave excitations of uniform and non-uniform targets modelled by geometrically accurate unstructured meshes. The method is demonstrated by comparing numerical results against analytical results.**

1 INTRODUCTION

The simulation of transient electromagnetic fields propagating through non-uniform penetrable objects positioned in free space has many important applications in physics, engineering and biomedical sciences. Modelling these transmission problems is challenging because of the presence of media characterized by complex and non-uniform material parameters and a large radiation environment.

Modelling these challenging processes requires the combination of volumetric and surface based numerical techniques. Among the time domain volumetric methods, the unstructured transmission line modelling (UTLM) technique is an appealing option. It is unconditionally stable, it allows for the description of a wide variety of materials and can be applied to general triangular unstructured grids [1]. The disadvantage of the UTLM method is the necessity to introduce approximate absorbing boundary conditions.

Among the surface oriented time domain techniques, the marching-on-in-time discretization of time domain boundary integral equations is appealing. The boundary element method (BEM) can model transient scattering from piecewise uniform objects and allows for the accurate and dispersion free description of outwardly radiating fields [2].

In this contribution, a boundary element unstructured TLM hybridisation (BEUT) is introduced that combines the advantages of both techniques to enable the modelling of scattering by complex materials and complex geometries whilst maintaining accurate free space boundary conditions.

In the past some early attempts have been undertaken to hybridize structured TLM and BEM methods [3–8]. However, these solvers cannot deal with unstructured grids and do not incorporate the recent advancements in the BEM that increase the stability and accuracy of the method. In addition, some of these techniques are conceptually complex and require the introduction of transitional padding layers or the use of discrete Green's functions.

After introducing the BEUT method and discussing its implementation, its efficiency and accuracy will be demonstrated by numerical examples.

2 THEORY

In this section the BEM and UTLM will be briefly revisited after which their hybridization is discussed.

2.1 BEM

The time domain representation formulas in operator form for the 2D transverse magnetic (TM) case can be written as [9]

$$\begin{pmatrix} \mathbf{e}_z \\ \hat{\mathbf{n}} \times \mathbf{h}_{xy} \end{pmatrix} = \begin{pmatrix} \frac{1}{2} + D & -\frac{\eta}{c} S \\ -\frac{c}{\eta} N & \frac{1}{2} - D' \end{pmatrix} \begin{pmatrix} \mathbf{e}_z \\ \hat{\mathbf{n}} \times \mathbf{h}_{xy} \end{pmatrix} + \begin{pmatrix} \mathbf{e}_z^i \\ \hat{\mathbf{n}} \times \mathbf{h}_{xy}^i \end{pmatrix} \quad (1)$$

where $\eta = \sqrt{\mu/\epsilon}$ is the characteristic impedance and $c = \sqrt{\mu\epsilon}$ is the wave propagation speed inside the medium. The tangential components of the electric and magnetic fields are denoted as $\mathbf{e}_z$ and $\hat{\mathbf{n}} \times \mathbf{h}_{xy}$ respectively, and superscript i denotes the incident field. The operators in eq. 1 are defined as

$$Du(\boldsymbol{\rho}', t) = \int_\Gamma \frac{\partial g(P,t)}{\partial n'} * u(\boldsymbol{\rho}', t)\ d\rho'$$

$$D'u(\boldsymbol{\rho}', t) = \int_\Gamma \frac{\partial g(P,t)}{\partial n} * u(\boldsymbol{\rho}', t)\ d\rho'$$

$$Su(\boldsymbol{\rho}', t) = \int_\Gamma g(P,t) * \frac{\partial}{\partial t} u(\boldsymbol{\rho}', t)\ d\rho'$$

$$Nu(\boldsymbol{\rho}', t) = -\int_t \int_\Gamma \frac{\partial^2 g(P,t)}{\partial n\, \partial n'} * u(\boldsymbol{\rho}', t)\ dn'\ dt$$

where g is the 2D time domain Green's function, $*$ denotes temporal convolution and $P = |\boldsymbol{\rho} - \boldsymbol{\rho}'|$. To reduce the order of the singularity contained by the

*George Green Institute for Electromagnetics Research, University of Nottingham, Nottingham, U.K.

hypersingular integrals in N, we apply the Green's identity to produce the combination of a singular contribution and a hypersingular contribution [10].

The formulation is discretized by expanding the fields as linear combinations of spatial/temporal basis functions, and then evaluating the equation at equidistant times (a.k.a collocation-in-time). The Lagrange interpolator [11] of the first order is used for the temporal basis functions, and the spatial signature of the electric and magnetic traces is described by rectangular pulses and linear hat functions, respectively.

2.2 Unstructured TLM

As derived by [1], the electric and magnetic fields on the faces of a triangle can be mapped onto the voltages and currents in an equivalent electrical circuit that has the same low frequency behaviour. As explained in [1], the Dirichlet-to-Neumann map for a small triangular region can be approximated in first order by a network of transmission lines with transmission time synchronised to the discretization timestep. The response of such a system to a pulse of width Δt can easily be computed analytically and provides the basis for UTLM.

Figure 1 shows a typical UTLM triangle. Each triangle is connected to its neighbour through ports via transmission lines, known as link lines, characterized by their length, propagation speed and impedance Z_{link}. In addition, stubs characterized by an admittance Y_{stub} are placed on each link line in order to accurately model the low frequency response of the medium. To ensure synchronisation of the transmission line network with the discretization timestep meshes must be Delaunay.

In order to match the inductive and capacitive response of the circuit to that of free space the transmission line parameters need to be chosen as

$$Y_{link_i} = \frac{l_i \Delta t}{2\mu\Delta_i}$$
$$Y_{stub_i} = \frac{\epsilon l_i \Delta_i}{\Delta t} - \frac{l_i \Delta t}{2\mu\Delta_i}$$

The link length and edge length associated with port i is given by Δ_i and l_i respectively. μ and ϵ respectively denote the permeability and permittivity of the medium associated with the triangle. To ensure that $Y_{stub_i} > 0$, thus minimising dispersion error, the following constraint exists on the timestep,

$$\Delta t < \triangle_{i_{min}} \sqrt{2\mu\epsilon} \tag{2}$$

The unknowns that are tracked in each triangle are the amplitudes of the left and right travelling waves (w.r.t some chosen orientation of the lines)

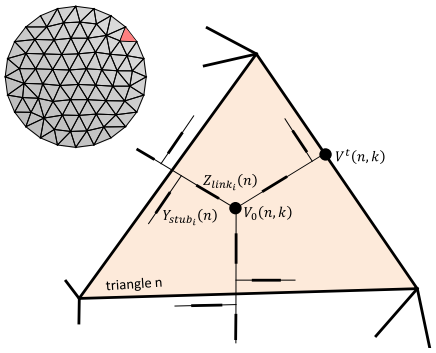

Figure 1: UTLM triangle.

on each link and stub line. These are updated at every timestep by considering local transmission line reflection and transmission problems as detailed in the next sections.

2.2.1 Scattering from the triangle centre

The scatter process refers to the computation of the reflected signals given the incoming signals at the triangle centre from all 3 ports.

To obtain the reflected voltage, we use the fact that the total voltage anywhere on a transmission line is the sum of the incident and reflected voltages. Since there is an open circuit at the end of a stub line, the incoming voltage simply gets reflected back.

$$\overline{V}^r_{link}(n,k) = V_0(n,k) - \overline{V}^i_{link}(n,k) \tag{3}$$
$$\overline{V}^r_{stub}(n,k) = \overline{V}^i_{stub}(n,k) \tag{4}$$

where superscript i and r denote the incoming and reflected voltages respectively, the overbar indicates a vector made up of values at all 3 ports, and $V_0(n,k)$ is the total voltage in the centre of triangle n at timestep k.

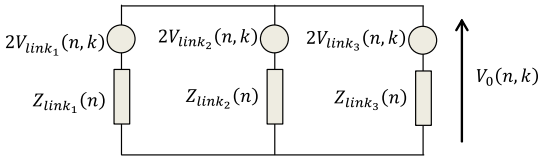

Figure 2: Thevénin equivalent circuit diagram of a UTLM triangle in the scatter process.

The total voltage at the centre of a triangle can be found using nodal analysis on the Thevénin

equivalent circuit (fig. 2)

$$V_0(n,k) = \frac{2\sum \overline{V}^i_{link}(n,k)\overline{Y}_{link}(n)}{\sum \overline{Y}_{link}(n)} \tag{5}$$

2.2.2 Connection between triangles

In the connect process the signals transmitted from one element to its neighbours are computed given the incoming signals at the inter-element edges. In structured TLM this step is trivial since pulses continue to travel unchanged to the neighbouring triangles. Due to the position of the stub lines in UTLM however the connect step is slightly more intricate.

Using nodal analysis and the fact that the total voltage is the sum of the incoming and reflected voltages, one can find the edge voltage between triangles m and n

$$\overline{V}^t(n,k) = \frac{2\sum\limits_{q=m,n}\left(\overline{V}^r_{link}(q,k)\overline{Y}_{link}(q) + \overline{V}^r_{stub}(q,k)\overline{Y}_{stub}(q)\right)}{\sum\limits_{q=m,n}\left(\overline{Y}_{link}(q) + \overline{Y}_{stub}(q)\right)}$$

The incident link and stub voltages for the next timestep is the difference between V^t and reflected values, which is then used in the scatter process in the next timestep, and thus the cycle repeats.

2.2.3 Connection at the boundaries

At the edges in the simulation domain boundary imbued with a local absorbing boundary condition the connect process is modified (fig. 3). The total voltage and current at the edge of the boundary triangle becomes

$$\begin{aligned} V^t_b(n,k) &= \frac{I^t_b(n,k)}{Y_{link_i}(n) + Y_{stub_i}(n) + Y_b} \\ I^t_b(n,k) &= 2V^r_{link}(n,k)Y_{link}(n) \\ &\quad + 2V_{stub}(n,k)Y_{stub}(n) \end{aligned} \tag{6}$$

For an approximate open boundary condition (accurate only for DC signals), the boundary impedance is set to be equal to the characteristic impedance

$$Z_{b_i} = \frac{V}{I} = \frac{\eta}{l_i} \tag{7}$$

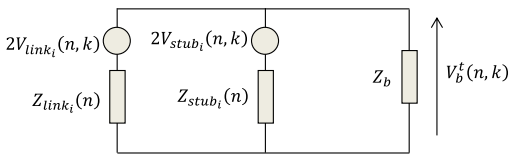

Figure 3: Thevénin equivalent circuit diagram of the boundary edge of a UTLM triangle.

2.3 BEUT

At the boundary of a UTLM model, we can use a generalisation of the equivalent circuit (fig. 3) by replacing the local boundary impedance with the BEM interaction matrix that couples all interface edges.

The closed circuit current and open circuit voltage at the boundary is

$$\begin{aligned} I_{closed} &= 2V^r_{link}Y_{link} + 2V^r_{stub}Y_{stub} \\ V_{open} &= \frac{I_{closed}}{Y_{TLM}} \end{aligned} \tag{8}$$

where the total admittance $Y_{TLM} = Y_{link} + Y_{stub}$.

This local circuit analysis allows to replace, for interfacing purposes, the combination of link line and stub with a single transmission line. The representation theorem for voltages and currents on this equivalent interface line reads

$$\begin{pmatrix} \mathbf{V}_b \\ \mathbf{I}_b \end{pmatrix} = \begin{pmatrix} \frac{1}{2} & \frac{Z_{TLM}}{2} \\ \frac{Y_{TLM}}{2} & \frac{1}{2} \end{pmatrix} \begin{pmatrix} \mathbf{V}_b \\ \mathbf{I}_b \end{pmatrix} + \begin{pmatrix} \frac{\mathbf{V}_{open}}{2} \\ -\frac{\mathbf{I}_{closed}}{2} \end{pmatrix} \tag{9}$$

where the matrices Y_{TLM} and Z_{TLM} are diagonal. The tangential fields at the boundary are related to the TLM unknowns by

$$\mathbf{e}_z \leftrightarrow \mathbf{V}_b \qquad \hat{\mathbf{n}} \times \mathbf{h}_{xy} l_b \leftrightarrow \mathbf{I}_b \tag{10}$$

where l_b is the boundary edge length.

Adding the representation formulas for the exterior domain (eq. 1) and the equivalent interface transmission line (eq. 9), taking into account the equivalences (eq. 10), results in the following convolution equation for the interface circuit unknowns

$$\begin{pmatrix} \mathbf{e}^i_z \\ \hat{\mathbf{n}} \times \mathbf{h}^i_{xy} l_b \end{pmatrix} + \frac{1}{2}\begin{pmatrix} -\mathbf{V}_{open} \\ \mathbf{I}_{open} \end{pmatrix} = \begin{pmatrix} -D & \frac{Z_{TLM}}{2} + \frac{\eta}{c} S l_b^{-1} \\ \frac{Y_{TLM}}{2} + \frac{c}{\eta} N l_b & D' \end{pmatrix} \begin{pmatrix} \mathbf{V}_b \\ \mathbf{I}_b \end{pmatrix} \tag{11}$$

where the first term is the exterior incident field contribution and the second term takes into account transmission line signals incident on the interface.

The BEUT method requires the following steps to be taken for every timestep:

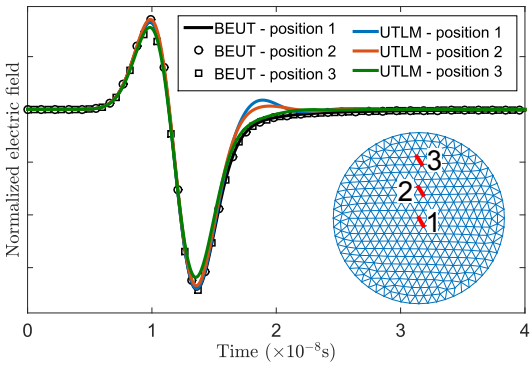

Figure 4: Results comparing traditional UTLM with the BEUT method when modelling free space.

1. Run the UTLM scatter process, then find $\mathbf{V}_{open}$ and $\mathbf{I}_{closed}$ using equation 8.

2. Solve the coupling equation 11 to obtain the boundary values.

3. Run the UTLM connect process using the updated boundary values.

The algorithm must adhere to the same timestep constraint proposed by UTLM in equation 2, which is likely to be small. This means that care must be taken when computing the BEM integrals near the singularities of the 2D Greens function. In some cases, the time step can be controlled by applying element merging techniques as described in [1].

3 RESULTS

As an initial verification, a 2D cylinder with a radius of 1m with the same characteristics as the background medium was meshed and excited with a point source in the interior of the cylinder, first using the traditional TLM matched impedance boundary conditions, and then repeated using the BEUT method. The propagation of the wave should be independent of the position of the source. Three different points in the cylinder were excited at distances 0m, 0.35m, and 0.7m from the origin and the electric field into the plane was observed at the same point. Using the matched impedance boundary condition at the boundaries gives conflicting results that are polluted by spurious reflections originating from the artificial simulation domain boundary. Using the BEUT method in contrast gives results that are not dependant on the exact location of the source and are not affected by spurious reflection, within reasonable discretization tolerance (fig. 4).

4 CONCLUSION

This paper has presented and demonstrated the boundary element unstructured transmission-line (BEUT) method, which is the hybridisation of the 2D time-domain boundary element method with the unstructured transmission line method.

The novel method has the ability to model complex materials with a plane wave source using an unconditionally stable technique in a domain that can be terminated with accurate radiating boundary conditions.

References

[1] P. Sewell, J. Wykes, T. Benson, C. Christopoulos, D. Thomas, and A. Vukovic, "Transmission-line modeling using unstructured triangular meshes," *IEEE Trans. Microw. Theory Tech.*, vol. 52, no. 5, pp. 1490–1497, 2004.

[2] Y. Beghein, K. Cools, H. Bagci, and D. De Zutter, "A space-time mixed galerkin marching-on-in-time scheme for the time-domain combined field integral equation," *IEEE Trans. Antennas Propag.*, vol. 61, no. 3, pp. 1228–1238, Mar. 2013.

[3] M. Zedler and G. V. Eleftheriades, "Anisotropic transmission-line metamaterials for 2-d transformation optics applications," *Proc. IEEE*, vol. 99, no. 10, pp. 1634–1645, Oct. 2011.

[4] S. Lindenmeier, L. Pierantoni, and P. Russer, "Adapted radiating boundaries (ARB) for efficient time domain simulation of electromagnetic interferences," *1998 IEEE MTT-S Int. Microw. Symp. Dig. (Cat. No.98CH36192)*, vol. 2, pp. 465–468, 1998.

[5] ——, "Hybrid Space Discretizing - Integral Equation Methods for Numerical Modeling of Transient Interference," *IEEE Trans. Electromagn. Compat.*, vol. 41, no. 4, pp. 425–430, Nov. 1999.

[6] ——, "Numerical modelling of transient radiated interferences in time domain by the hybrid ARB method," *Int. J. Numer. Model. Electron. Networks, Devices Fields*, vol. 12, no. 4, pp. 295–309, Jul. 1999.

[7] S. Lindenmeier, C. Christopoulos, and P. Russer, "Methods for the modeling of thin wire structures with the TLM method," *2000 IEEE MTT-S Int. Microw. Symp. Dig. (Cat. No.00CH37017)*, vol. 1, pp. 387–390, 2000.

[8] L. Pierantoni, S. Lindenmeier, and P. Russer, "A Combination of Integral Equation Method and FD/TLM Method for Efficient Solution of EMC Problems," *27th Eur. Microw. Conf. 1997*, vol. 2, pp. 937–942, 1997.

[9] Y. Beghein, K. Cools, F. P. Andriulli, D. De Zutter, and E. Michielssen, "A calderon multiplicative preconditioner for the PMCHWT equation for scattering by chiral objects," *IEEE Trans. Antennas Propag.*, vol. 60, pp. 4239–4248, 2012.

[10] G. C. Hsiao and W. Wendland, "Boundary Integral Equations," in *Theor. Numer. Anal.* Berlin: Springer, 2008.

[11] B. Shanker, A. Arif Ergin, K. Aygün, and E. Michielssen, "Analysis of transient electromagnetic scattering phenomena using a two-level plane wave time-domain algorithm," *IEEE Trans. Antennas Propag.*, vol. 48, no. 4, pp. 510–523, 2000.